A Priority-Based Scheduling Scheme for Search, Track, and Communications in MPARs

Augusto Aubry, *Senior Member, IEEE*, Antonio De Maio, *Fellow, IEEE*, and Luca Pallotta, *Senior Member, IEEE*

***Abstract*— The modern battlefield scenario is strongly influenced by the innovative capabilities of multifunction phased array radars (MPARs), which can perform a plethora of sensing and communication (COM) activities sequentially or in parallel. In fact, the MPAR can functionally cluster its phased array into bespoke subapertures implementing different tasks. Accordingly, a portion of the other available resources, e.g., bandwidth, power-aperture product (PAP), and time, is also assigned to each subaperture, and the grand challenge is the definition of strategies for optimal scheduling of the tasks to be executed. In this respect, a rule-based algorithm for task scheduling is proposed in this article. In a nutshell, in each time window, the procedure first allocates the radar tasks (viz., volume search, cued search, update, and confirmation tracking) and then utilizes the COM looks to fill the empty intraslot time left by the radar tasks. When there are two concurrent looks, the allocation is performed according to their priorities. Moreover, if the bandwidth and PAP are sufficient, some of them can be also scheduled in parallel. Interesting results in terms of bandwidth and time occupancy efficiency are observed from simulations conducted in challenging scenarios comprising also multiple maneuvering targets.**

***Index Terms*— Dynamic resource allocation, multifunction phased array radar (MPAR), rule-based algorithm, task scheduling.**

I. Introduction

RECENT years have experienced the evolution of both military and civilian radars toward the implementation of multifunction phased array radar (MPAR) systems. This is essential because this kind of architecture can perform (also at the same time) a plethora of activities, thanks to the provision of simultaneous beams. In fact, an MPAR system can perform operations that, in the past, were demanded to separate radars. Indeed, the system is capable of functionally clustering the aperture array into several subapertures and piloting them independently to each other. In such a way, the multifunction phased array radar (MPAR) further expands the flexibility of the phased array, by enabling it to electronically steer many beams in different directions, while transmitting different waveforms each designed to reach a specific goal. To do this, the MPAR necessitates a radar resource manager (RRM), whose aim is to effectively and appropriately manage the diverse functionalities, ranging from target search to target tracking, classification, and/or communications (COMs), just to list a few [1]. For an efficient use of the resources, the system needs to continuously probe and glean knowledge about the operating environment before performing an adaptive setting of the involved parameters and resources [2], [3], [4].

The RRM is responsible for an optimal allocation of the limited radar resources (e.g., bandwidth, power-aperture product (PAP), and time) to each demanding function (or task associated with them) [5]. This is done based on two competing factors, viz., the finite availability of resources and the satisfaction achieved in effectively performing a specific operation according to its importance for the overall MPAR mission (in fact, some functions are more mission-critical than others). Therefore, in order to properly weigh the respective importance and sensitivity of the involved functions, the RRM must assign some bespoke priorities to each of them (e.g., on the basis of the threat level of the activity). Not surprisingly, the design and development of complex algorithms for resource allocation are demanded to fulfill the mentioned challenges [3], [4]. Specifically, the resource allocation strategies implemented in the RRM must efficiently share the overall amount of each limited resource for all the functions/tasks while honoring their performance constraints. Clearly, being the tasks in competition with each other for the resource assignment, the RRM must adaptively establish the optimal distribution that allows to guarantee the maximum satisfaction of the final MPAR mission, sacrificing lower priority tasks in favor of the higher. Notably, the resource allocation problem is also gaining attention in the integrated sensing and communication (ISAC) context [6].

The resource allocation process can be done by following different strategies, such as the quality of service resource allocation method (Q-RAM) [1], [7], [8], [9], [10], [11], [12], [13], [14], the continuous double auction parameter selection (CDAPS) [3], [15], [16], [17], [18], and/or quality-of-service (QoS)-based algorithms [4], [18], [19], [20]. In particular, the Q-RAM is an iterative procedure that increasingly assigns the resources to each task in decreasing order in terms of

Manuscript received 19 January 2024; revised 25 March 2024; accepted 25 April 2024. Date of publication 29 April 2024; date of current version 9 May 2024. The work of Augusto Aubry and Antonio De Maio was supported by European Union through Italian National Recovery and Resilience Plan (NRRP) of NextGenerationEU, partnership on "Telecommunications of the Future" (PE00000001—Program "RESTART"). *(Corresponding author: Antonio De Maio.)*

Augusto Aubry and Antonio De Maio are with the Department of Electrical Engineering and Information Technology (DIETI), Università degli Studi di Napoli Federico II, 80125 Naples, Italy, and also with National Inter-University Consortium for Telecommunications, 43124 Parma, Italy (e-mail: augusto.aubry@unina.it; ademaio@unina.it).

Luca Pallotta is with the School of Engineering, University of Basilicata, 85100 Potenza, Italy (e-mail: luca.pallotta@unibas.it).

Digital Object Identifier 10.1109/TRS.2024.3394896

marginal utility until all the available resources are allocated. On the contrary, the CDAPS implements the continuous double auction (CDA) market algorithm [21], with the tasks modeled as agents to which a certain amount of resource is associated together with a limit on the overall budget of the specified resource. Differently, the algorithms based on QoS optimization formulate a constrained optimization problem, where the limited resource (e.g., PAP) is appropriately shared to maximize the overall QoS. Finally, other resource assignment methodologies have been developed in [22], [23], and [24], where the allocation problem is addressed following a Bayesian framework and consists in selecting the best sensing mode that minimizes the uncertainty in the threat level of the targets.

Beyond the above-mentioned resource distributions, it is worth underlining that the RRM should also perform scheduling of the tasks for being executed over time. In fact, during the resource distribution process, due to the limited budget, some tasks cannot be allocated in the current time slot (also known as update interval or time window) under consideration and should be scheduled in the next time slots. In particular, for each update interval, the radar tasks create one or more look requests involving a specific amount of resources to reach their objective. In this respect, the RRM should establish a timeline that describes the tasks to execute inside each update time, defining their starting time, duration, and the resources they will employ. The timeline can be hence created following different strategies [25], [26], [27], [28], [29]. The method designed in [25] and [26], also known as time-balancing, was implemented in the experimental multifunction electronic scanned array radar (MESAR) system developed by QinetiQ and AMS Ltd. Its idea consists in assigning to each look a time balance. Then, the scheduling is made based on this value. In fact, the following three different situations can arise: 1) a zero time balance means that a look must be executed immediately; 2) a negative time balance corresponds to a look that cannot be executed; and 3) a positive value indicates the time instance at which the look should be executed. Then, tasks are executed in sequence, according to their priority as well (if any). By doing so, the time efficiency can be quite close to 100%. An alternative method is the so-called coupled-task scheduler [27], which is based on the exploitation of the separation time between the two consecutive operations, where an additional task is possibly inserted to occupy the residual time to boost efficiency.

Regardless of the employed scheduling method, a fundamental subproblem should be first addressed. It consists in properly ranking the task's priority values assignment [1], [3], [30], [31]. Currently, different strategies toward this goal can be clustered into two different groups, viz., rule-based versus fuzzy logic-based [1], [3], [32], [33]. In the first case, the priority assignment is done by defining the importance (e.g., threat) as well as the sensitivity of each task with respect to the overall mission, and fixed priority values are typically assigned [3]. The other class of approaches relies on the use of fuzzy values that are assigned to variables representing attributes of the specific tasks. Hence, an if-then rule can used to determine the priority of each task [32], [33].

In [31], an example of tasks scheduling based on a rule-based priority assignment for an MPAR performing volume search, cued search, and tracking is provided. Specifically, at each update time, the scheduler organizes the look requests accounting for their starting time and privileging those associated with tasks of higher priority (for concurrent looks). The considered limited resources to be shared are hence the bandwidth, PAP, and time. According to the bandwidth and PAP requirements, volume and cued search could also be performed in parallel, whereas tracking is greedy and demands all the available resources during its execution. The major drawback of this approach is that the time resource is not exploited most efficiently. In fact, in each update interval, a certain amount of time might remain unused.

To overcome the above limitation, in this article, a framework that expands [31] by integrating communication (COM) tasks together with radar sensing is proposed. Note that the coexistence and integration of sensing and COM operations is becoming one of the hottest research topics within both the radar and COM community [34]. It can be realized by following diverse strategies such as *time-division access* (e.g., alternating operation), *frequency-division access* (e.g., spectrum sensing), *code-division access* (e.g., orthogonal waveforms), and/or *space-division access* [34], [35]. Hence, the proposed strategy (which is radar-centric) consists of a *rule-based* approach, which allocates COM looks to fill the gaps left by the radar tasks in the update interval. In fact, the scheduler first allocates the higher (radar) priority tasks and then utilizes COM operations to increase the effectiveness in the usage of the time resource. In more detail, the COM tasks share the lowest priority assignment, but they are carried out in parallel to volume search tasks (satisfying the resources constraints) whenever a cued search is not executed. Moreover, they are allocated in the idle times left blank in each update time by the radar operations. Nonscheduled tasks (referred to as deferred tasks) are delayed to be considered for the next update intervals after their priority is increased (except for the COM ones). It is finally worth observing that the algorithm adaptively chooses the revisit time for the tracking tasks based on some useful metrics (e.g., track sharpness and model's probability). Some simulations in scenarios of practical interest demonstrate the effectiveness of the proposed strategy with a substantial increment in the effectiveness of the used bandwidth and time resources.

Summarizing, the main contributions of this work are as follows.

1) The generalization of the framework of [31] contextualizes it in ISAC applications, where both sensing and COMs capabilities are somehow integrated, thus enlarging the application to a much broader set of operating contexts.
2) Definition of new specific metrics (viz., the channel capacity per bandwidth and the range at which it is guaranteed) to account for COM tasks that substantially differ from those of the sensing tasks.
3) Wise exploitation of COM tasks to overcome the drawbacks of the method in [31], which does not fully capitalize on the available resources in terms of both

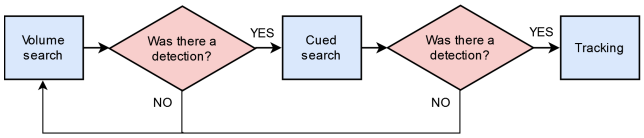

Fig. 1. Operative principle of look request activation for cued search and tracking under detection events occurrence.

bandwidth and time. Therefore, COM operations are interlaced in order to recover wasted resources from sensing operations and, hence, used as bandwidth and time gap fillers.

4) Extensive simulations, conducted also in comparison with the algorithm of [31], highlighting the practical effectiveness of the proposed framework.

This article is organized as follows. In Section II, some preliminary concepts on the MPAR system are provided, and the problem of limited resource allocation is introduced. In Section III, a description of the considered task scheduling problem is given together with the definition of the involved resources to share between the radar and COM tasks. The devised algorithm is then illustrated in Section IV and analyzed on a simulated scenario of practical importance in Section V. Finally, some conclusions are drawn in Section VI with possible hints for future research directions.

II. Preliminary Concepts

In this article, we consider an MPAR system capable of performing three radar tasks, i.e., volume search, cued search, and tracking, while performing COMs with other devices or users. In this multitask scenario, exploiting the dynamicity and flexibility of its active electronically steered array (ESA) antenna, the MPAR can steer a multitude of beams in different directions each of them devoted to a specific task. Therefore, the system must reserve for each task a part of the available resources in terms of bandwidth, PAP, as well as the execution time. Assuming a scenario comprising multiple (generally maneuvering) targets, at each update interval, each task needs a certain amount of the aforementioned resources from the MPAR to appropriately accomplish its goal, e.g., to perform searching for targets, track one or more targets, and convey communication (COM) information. Along the time, each task produces one or more look requests that include the amount of demanded resources for being effectively executed. However, some look requests are activated upon the occurrence of some events triggered by other tasks. The operative principle of the look request activation flowchart is illustrated through the scheme of Fig. 1.

More precisely, the volume look requests are continuously activated in order to perform the scan of a large volume of space. After the volume search is performed, if detection occurs, the resulting target detection is sent back to the processing unit, where a cued look request is generated. This sequential process is performed since the detections obtained by the volume search offer approximate target locations that are then refined by the bespoke cued search looks. In fact, the volume search task usually exploits a wide beam and a narrowband waveform to reduce the total search time. Then, the cued search allows the MPAR to address surveillance adaptively by scanning a small region around a detection produced by the volume search. To this end, the cued search relies on a narrower beam and a wider bandwidth for better accuracy. Similar to the volume search, when a detection is produced by the cued process, it is passed to the tracking task. Here, two competing situations can arise. On the one hand, if it is not possible to associate the confirmed detection to any existing track, a new target track is created. In such a case, the tracking task initiates an unconfirmed track and requests a so-called confirmation look. On the other hand, if the confirmed detection is associated with an existing track, the tracking task actuates the request for a track update look. It is worth underlining that the tracking is performed in an adaptive fashion. In fact, the tracks are updated based on some parameters that are related to the target dynamics (e.g., if there is the presence of a maneuvering or not-maneuvering target as well as its threatening level). Finally, COM look requests are continuously activated, and executed each time if there are some usable resources, following the criteria specified in Section IV. Depending on the amount of resources required by each involved task, at each update interval, the MPAR can execute different tasks sequentially or in parallel (if two or more tasks can share the available resources without affecting/impairing the success of their mission).

III. Problem Description

A fundamental requirement of the MPAR to execute different tasks in parallel is its capability of partitioning its phased array into several subarrays. By doing so, it can create multiple simultaneous beams with different values of PAP associated with each of them.[1] Moreover, it can change the transmitted waveform parameters, hence having the potentiality of transmitting different signals at the same time. However, each radar task requires access to some amount of bandwidth, PAP, and time resources. Therefore, due to practical and physical constraints on the available resources, the involved tasks must compete with each other in order to get them. Hence, the MPAR organizes the tasks to be executed in the upcoming time window, say $[t_k, t_{k+1}]$, with k being the time index. It is tantamount to underlining that, for each update interval, a radar task produces one or more look requests in terms of resources necessary to reach its objective; these requests strictly depend on the current operational situation (i.e., the scenario, the number of targets, and their positions) as better specified in the remaining part of this article. Once a radar look is produced, it incorporates several information useful to properly allocate the resources. The MPAR must acquire knowledge about the type of waveform to be used

[1] In the proposed architecture, the antenna array is divided into spatially separated subarrays (i.e., a spatial division multiplexing is performed) to generate multiple beams. Moreover, each subaperture is fed by the T/R modules of its elements that transmit the waveform dedicated to a specific function. In addition, in order to induce isolation between the separated beams, it is assumed that frequency orthogonal waveforms are used. Nevertheless, to further reduce the possible interference between sensing and COMs functions, orthogonal (or quasi-orthogonal) codes can also be superimposed on different carrier frequencies.

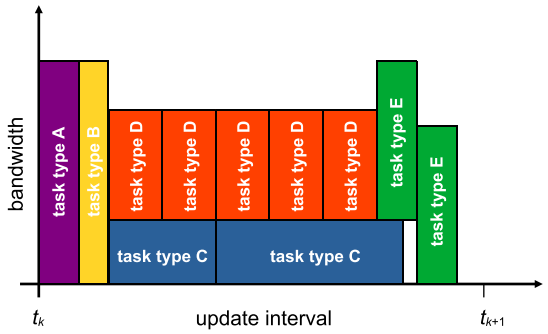

Fig. 2. Notional example of the MPAR scheduling of different tasks sharing the bandwidth resource in a generic update interval. The same color refers to different looks of the same task.

(e.g., bandwidth and transmitting power) as well as about the beam to produce (e.g., steering angle, dwell time, and subarray size). Then, the RRM organizes all the generated looks in a possible timeline based on a specific scheduling algorithm as detailed in Section IV.

To provide an insight into this approach, Fig. 2 shows a notional example of task scheduling. Five different task typologies sharing the bandwidth resource are organized in a generic update interval. From the figure, the evidence is that the scheduler organizes different task looks in order to satisfy their bandwidth requirements according to the overall availability of the shared resource.

The RRM creates a timeline composed by consecutive update times, each of them containing the scheduled looks, in turn, characterized by their own starting time and duration (as defined by each specific dwell). Therefore, once the timeline for the next update interval is completed, the RRM moves the not-scheduled looks into a list of *deferred tasks*, which will be considered for possible planning in the next update interval. How to manage the deferred looks depends on the specific scheduling algorithm. More details about this aspect are reported in Section IV.

A. System Resources

As already pointed out, in this article, the bandwidth, the PAP, and the time duration are considered as the limited resources to be shared among the tasks.

The bandwidth of the transmitted signal depends on the resolution required by a specific radar task. Hence, in this work, it is assumed that the tracking requires the entire bandwidth available at the MPAR for its execution. On the contrary, for the cued search, a lower bandwidth is needed, whereas the volume is the task with the lowest requirements in terms of bandwidth. Finally, as to the COM operations, a distinct strategy is herein followed. Practically, the bandwidth associated with COM operations is statically set such that it can be also executed in parallel to a volume task. The reason for this choice will be clarified during the explanation of the scheduling algorithm in Section IV.

The second considered limited resource is the PAP that is defined as the product of the average transmitted power, say P_{av}, and the aperture size, A_e, of the activated subarray. With reference to the hth subarray used to accomplish the hth task, it is [36]

$$\text{PAP}_h = P_{\text{av}}^h A_e^h = P_t^h \tau \text{PRF} A_e^h \tag{1}$$

where P_t^h is the peak transmitted power for the hth subarray, τ is the pulse duration (or pulsewidth), and PRF is the pulse repetition frequency of the burst.

Finally, it is worth recalling that each look requires a different duration depending on several endogenous and exogenous factors, e.g., detection performance as well as waveform and target characteristics. Clearly, different looks can be served in parallel, when they can share all the other resources. However, if this is not the case, they must be executed sequentially in the same or in different update intervals, depending on the compliance of their durations with the overall update window size. For these reasons, it is of paramount importance for the RRM to compute the time duration for each task as well as figure out the overlaying possibilities before organizing them in the timeline. Being the update window of fixed duration, some looks will be scheduled and executed at the update interval under planning, whereas the remainder will be postponed. As to the radar tasks, the execution time required by each look is given by the dwell time that is defined as the product of the number of pulses in the burst and their pulse repetition interval (PRI). Hence, denoting by $D_x(P_d, P_{\text{fa}})$, the radar detectability factor (i.e., a quantity determining the received signal energy needed to achieve the desired probability of detection P_d given the probability of false alarm P_{fa} computed for unit noise power [31]), the number of transmitted pulses for each radar look can be computed from the radar range equation as follows [36]:

$$n = \left\lceil \frac{(4\pi)^3 k_B T_s D_x(P_d, P_{\text{fa}}) R^4 L_s L_h(\theta, \phi)}{P_t^h \tau G_h^2 \lambda_0^2 \sigma} \right\rceil \tag{2}$$

where $k_B = 1.38 \times 10^{-23}$ J/K is the Boltzmann constant, T_s is the system noise temperature, R is the target range, G_h is the gain of the subarray that depends on the azimuth and elevation beamwidth, λ_0 is the operating wavelength, and σ is the target radar cross section (RCS). The function $\lceil \cdot \rceil$ provides the smallest integer greater than or equal to its argument. Finally, L_s indicates the overall system loss, whereas $L_h(\phi, \theta)$ is the term accounting for the scanning gain loss of the steered antenna due to scanning off boresight in the pointing direction (ϕ, θ) (with ϕ being the azimuth and θ being the elevation), that is [31],

$$L_h(\phi, \theta) = \cos^{-3}(\phi) \cos^{-6}(\theta). \tag{3}$$

The scan loss is a deleterious effect that impacts the evaluation of the number of pulses needed to ensure the same detection performance for different search looks. As a consequence, when the radar points off-boresight, a higher number of pulses (namely, a waveform diversity) is needed to compensate for the mentioned loss.

B. Volume and Cued Search Tasks

Volume search scans the volume of interest to detect a possible target. Each look of this task is characterized by a given pointing direction within a grid of directions based on

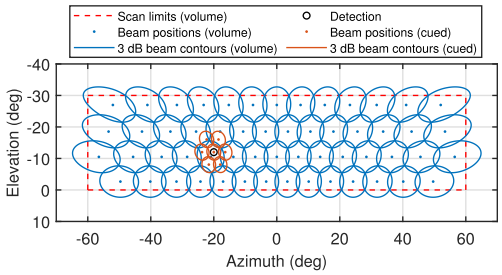

Fig. 3. Search grid with volume and cued 3-dB beams.

which beam and waveform features are established accordingly too. In particular, to accomplish a wide region scanning, the volume task is characterized by a wide beam and a low bandwidth. Then, if during a volume search, a detection is triggered, the related measurements feed the processing unit that will initialize the cued search task. Specifically, a cued search look is demanded that, beyond the proper waveform and beam characteristics, consists of seven (or five if the detection is on the edge of the search volume) beams that should be sequentially transmitted (due to bandwidth limitations) in order to refine the search around the specific direction, where the volume has triggered a detection. In this respect, the cued search is characterized by a narrower beam and a wider bandwidth than the volume one. Now, if the cued search confirms the detection, the respective measurements are passed back to the processing unit that will activate the tracking process (whose functionalities are described in Section III-C). To help readers toward a better understanding of these concepts, in Fig. 3, the entire search grid is shown together with the 3-dB beams transmitted for both the volume and cued search tasks. It is worth noting that to reduce the straddling loss, the adjacent volume search beams have been slightly overlapped.

C. Tracking Task

The tracking task, along with the conventional looks requested to feed the already formed tracks, generally, comes into play when a detection is obtained during the cued search process. It can accomplish two operating functions depending on the specific situation that arises. In fact, it can require the production of two alternative looks. The former is referred to as track confirmation and is activated when the detection coming from the cued task cannot be associated with any other existing tracks. When this is the case, the tracking task must initiate a new unconfirmed track through the request of a confirmation look. On the contrary, if the measurement associated with the cued detection can be associated with an existing track, the tracking task proceeds with a track update look request. Clearly, this dual structure assumes that different parameters will be involved in the two alternative tasks. The confirmation looks can be considered a more important task than the update one, and hence requires a revisit time that should be done as soon as possible. To obtain a confirmation of the track, a logic based on an M-of-N threshold is used (in the simulations conducted in Section V, it is set $M = 3$ and $N = 5$).

The tracker is based on an interacting multiple model (IMM) filter that is designed for highly maneuvering targets. In fact, the IMM filter deals with the multiple motion models according to a Bayesian framework [36], [37], [38], [39]. Specifically, this method resolves the target motion uncertainty by jointly using multiple models at a time for a maneuvering target. All of them are simultaneously used to come up with a combined state estimate. In particular, the considered tracker uses two extended Kalman filters (EKFs) in parallel particularized for two different motion models. The former is a constant velocity model (i.e., for a nonmaneuvering target), whereas the latter is the so-called constant turn (for a maneuvering target), which describes a motion in the xy plane with a constant angular velocity and in the vertical direction with a constant velocity. The final state estimate is obtained as a combination of the two state filter outputs, as well as exploiting the model probabilities and the model switching probabilities. Precisely, the probability that a model is active can be evaluated from the measurement innovations. Hence, the estimates and error covariances for all models are approximately mixed [36]. In the case studied in this article, the model transition probabilities are set equal to 0.99 for both models.

Finally, when the tracking task requests a track update look, it finds the track revisit rate adopting one of the following three adaptive strategies.

1) Adaptive Revisit Time Based on Track Sharpness: The track revisit rate is chosen as the lowest revisit rate at which the predicted azimuthal track accuracy (viz., the azimuth standard deviation, σ_c) does not exceed a preassigned threshold [1], [4], [40]. In particular, the threshold is chosen equal to a fraction of the beamwidth in azimuth, that is, the beamwidth in the azimuth direction multiplied by the track sharpness (normalized azimuth accuracy), namely,

$$\sigma_c < \eta_0 \cdot \mathrm{BW}_\phi \tag{4}$$

where η_0 is the dimensionless track sharpness parameter, which controls the maximum allowed inaccuracy of the track in relationship to the azimuth beamwidth BW_ϕ.

2) Adaptive Revisit Time Based on Estimated Maneuver: This method consists in choosing the revisit time as a function of the target maneuver. In particular, if the model probability for the maneuvering model is greater than a predefined value ($P_m > 0.5$ is used in the simulations conducted in this article), the revisit time is chosen equal to the lowest possible, differently it is selected as the highest possible. This is because a maneuvering target could be lost during the tracking update process if the revisit time is not sufficiently short.

3) Adaptive Revisit Time Based on NEES: The accuracy of the covariance is measured through the normalized estimation error squared (NEES) that, for a single sample in the case of constant velocity estimate, should be chi-square distributed with six degrees of freedom [36], [38]. Hence, the average value for the NEES should be 6, where the confidence interval for the chi-square distribution is $[\xi_{\mathrm{L}}^2, \xi_{\mathrm{H}}^2]$. For instance, the interval [0.87, 16.81] is derived by setting the confidence to 98%. As a consequence, the revisit time can be set as the maximum revisit such that the estimated NEES is within a specific interval $[\xi_{\mathrm{L}}^2, \xi_{\mathrm{H}}^2]$.

It is finally worth noticing that, for all the above-mentioned strategies, the tuning parameters (viz., η_0, ξ_{L}^2, ξ_{H}^2, and P_m)

should be set according to the knowledge about the riskiness of the operating environment. Moreover, similar results can be achieved by the above three methods through a proper choice of the tuning parameters.

D. COM Task

In addition to sensing operations, it is assumed that the MPAR could communicate with many U users and/or devices. Hence, the system can transmit a signal given by the superposition of U frequency (or code) orthogonal waveforms, $x_i(t)$, $i = 1, \ldots, U$. As for the radar tasks, when the COM task requests a look, first, the pointing angle is defined, and the beam and waveform properties are derived consequently. The PAP being a limited resource, it can be adaptively chosen rather than a priori fixed. In particular, once the COM range is chosen, it can be set as the value such that the channel capacity per bandwidth is equal to a specific value.

Assuming an additive white Gaussian noise (AWGN) channel, from the Shannon–Hartley theorem, the channel capacity per bandwidth (expressed in bit/s/Hz) for the kth user is [41], [42], [43]

$$C_k = \log_2\left(1 + \mathrm{SNR}_k^{\mathrm{COM}}\right) \tag{5}$$

where $\mathrm{SNR}_k^{\mathrm{COM}}$ is the signal-to-noise ratio (SNR) at the kth COM user receiver. Hence, indicating with $R_{k,\mathrm{COM}}$ the range at which the user is located, the SNR is given by [19]

$$\mathrm{SNR}_k = \mathrm{PAP}_k \frac{A_e^{\mathrm{rx},k}}{\lambda_0^2 R_{k,\mathrm{COM}}^2 L_s^{\mathrm{COM}} L_{\mathrm{steer}}^{\mathrm{COM}} k_B T_s^{\mathrm{COM}} B^{\mathrm{COM}}} \tag{6}$$

where $A_e^{\mathrm{rx},k}$ is the effective area of the kth user receiving antenna, L_s^{COM} is the COM system operational loss, $L_{\mathrm{steer}}^{\mathrm{COM}}$ is the scanning loss in the COM scenario, B^{COM} is the bandwidth available in the MPAR for COM operations, and T_s^{COM} is the noise system temperature.

Finally, denoting by C_{desired} the reference value for the objective channel capacity, the PAP that allows to reach this capacity, say $\overline{\mathrm{PAP}}_k$, is derived as follows:

$$\overline{\mathrm{PAP}}_k = \frac{\left(2^{C_{\mathrm{desired}}} - 1\right)\lambda_0^2 R_{k,\mathrm{COM}}^2 L_s^{\mathrm{COM}} L_{\mathrm{steer}}^{\mathrm{COM}} k_B T_s^{\mathrm{COM}} B^{\mathrm{COM}}}{A_e^{\mathrm{rx},k}}. \tag{7}$$

Before concluding this section, it is worth recalling that different types of COMs can be performed. For instance, the MPAR could send some tactical information to soldiers, and/or to other radar or electronic warfare (EW) infrastructures that are in the same area, as well as to moving vehicles like unmanned aerial vehicles (UAVs). Finally, it can implement a wireless network by acting as a router when the civilian one is inhibited.

IV. Task Scheduling Algorithm

The scheduling algorithm adopted in this article starts from the assumption that the possible available resources cannot be allocated at any time to the required tasks. In fact, each task subsumes a dynamic process that for each update interval can demand one or more looks depending on the current situation. Hence, a radar look should contain information about the pointing direction of the MPAR beam, its bandwidth, the PAP, as well as its nominal start time and related duration.

In the context of this article, as in [31], it is assumed that the tracking tasks require all the available bandwidth and PAP, and hence, they cannot be executed in parallel to any other task. Differently, the volume search, cued search, and COM tasks call for a reduced amount of resources both in terms of bandwidth and PAP than the tracking. In particular, the volume requires a quite low bandwidth and PAP, making it a candidate to be executed in parallel with cued search and COM tasks, as described later.

For the above-mentioned reasons, the mechanism at the base of the considered scheduling algorithm makes use of priorities assigned to each task, in terms of a number ranging from 5 (very high priority) to 1 (very low priority). Hence, the RRM allocates the temporal resource according to the required start times while respecting the prioritization. Moreover, in the case both PAP and bandwidth can be simultaneously shared between two tasks, they can be also scheduled for being executed in parallel. In the scenario studied in this article, the priorities are assigned as 5 for track confirmation, 4 for track update, 3 for cued search, 2 for volume search, and 1 for COM. As to the latter, the algorithm operates in a different way as compared with radar tasks. In fact, COM tasks are allocated in parallel to volume search (taking care of not violating the constraints on resources) each time the cued search is not performed. Moreover, COM looks are also allocated in order to fill the gap in the update interval left by the other radar tasks (e.g., in the intraslot time). Finally, it is also worth underlining that all the tasks that are not allocated for being executed in the incoming update interval, as nominally desired, are organized in a list of deferred tasks. The deferred tasks experience a modification in their priority that is increased by a factor of 0.25 and will be planned to be executed in the successive updates. Differently, the priority of the deferred COM is not modified since the COM mission is less relevant than the radar mission (radar-centric approach). The principle adopted by the highest priority scheme is provided in the left part of Fig. 4, whereas the entire procedure herein developed is notionally illustrated in its right part.

The flow diagram shown on the left side of Fig. 4 is the so-called high-priority typology, whose working principle can be described as follows. Taking the list of tasks, they are first sorted in decreasing order by priority; then, the ordered tasks are sequentially (or in parallel if there is margin in terms of availability of the physical resources) scheduled in order to fill the time window. Finally, if all the tasks have been scheduled, the process ends; otherwise, the remaining tasks are moved in a list of deferred actions with their priority increased by an amount of 0.25 (except for the COM tasks whose priority level is maintained unaltered).

Now, it is worth going further into the details of the proposed strategy, with reference to the block scheme in the right part of Fig. 4. The algorithm begins acquiring all look requests from the tasks whose starting time falls in the current update window. Then, it extracts from that list the confirmation tracking looks, being the tasks with the highest priority. Hence,

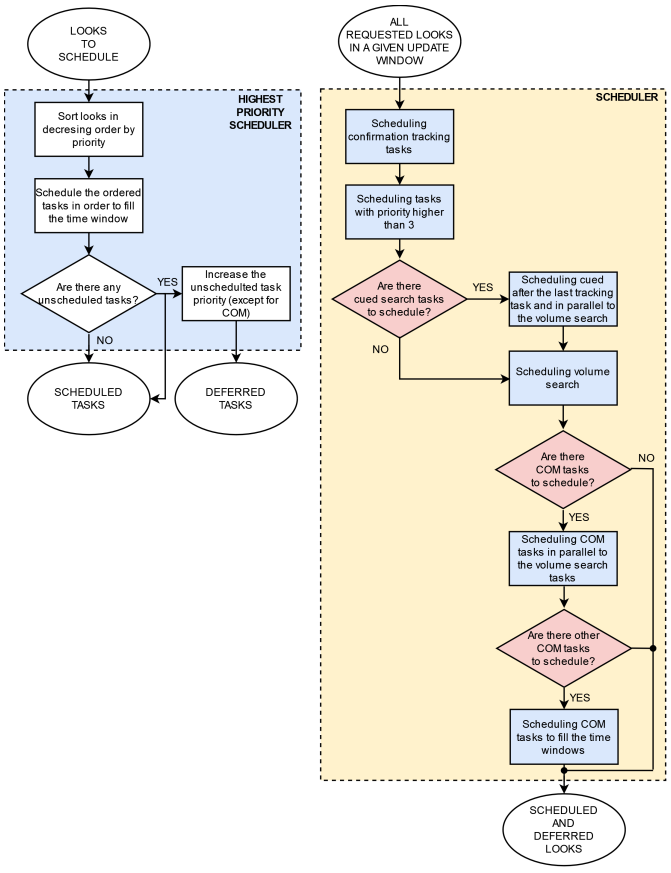

Fig. 4. Proposed algorithm for task scheduling in an MPAR system performing volume search, cued search, tracking, as well as implementing a COM functionality.

the tracking looks are scheduled in order to turn on the filling process of the update interval. If confirmation tracking looks are no longer present (they have been already scheduled or completely absent), and there is a temporal margin to encapsulate other looks in the update interval, the RRM continues the analysis of the look requests list. At this point, the RRM schedules looks with a priority higher than 3 (according to their priorities), which could be both update tracking tasks as well as other deferred radar tasks. After that, the RRM checks for the presence of a cued search in the list. If they are present, they are scheduled just after the tracking looks (if any) and in parallel to possible volume search looks. Clearly, once a certain number of tasks have been allocated, if the remainder tasks have a duration that is not compliant with the residual time until the end of the update window, they are moved to the list of deferred tasks (as shown in Fig. 4). It is worth mentioning that the volume search tasks are usually scheduled sequentially even in the absence of cueds. In fact, in general, it could be not necessary to increase the scan rate of the search grid for typical detection scenarios [36]. However, when there are multiple track operations, volume tasks could be also done in parallel. Once the radar task scheduling is terminated, the RRM involves in the completion of the update interval of the COM tasks. As a matter of fact, according to the choice of the constraints on the available resources, COM looks are assigned to be executed in parallel to all volume search tasks which otherwise would have been executed alone, or when there is sufficient empty space, COM looks are scheduled starting at the end time of the allocated radar tasks. More precisely, COM looks are used to fill the gap between the radar tasks and the end of the update interval, in order to exploit in the possible best way the timeline. Clearly, COM tasks that are not allocated are also added to the list of deferred tasks.

Finally, it is worth observing that it is not excluded that a more efficient rule for resource allocation can be found; however, the proposed rule-based scheme is simple and has shown interesting performance as shown in Section V. For instance, volume tasks could be executed in parallel depending on the quantity of bandwidth and PAP resources they require. In particular, there could be situations in which, due to an unexpected overload, the radar would find it wise to execute in parallel some volume tasks to reestablish a desired timeline. It is also worth pointing out that a situation of practical relevance in which it is preferable to avoid the execution of volume search in parallel arises when harvesting energy is required, for instance, when it is demanded to probe the environment with a burn-through waveform. Clearly, the designer can perform the most suitable choice depending on the specific missions and environments.

V. Results

This section is devoted to analyze the results of the devised resource allocation algorithm described in Section IV.

Tests conducted in this article refer to a long-range MPAR operating in the *S*-band with its operating central wavelength $\lambda_0 = 0.09$ m. The analysis is conducted considering a radar scenario involving the presence of several maneuvering radar targets and trajectories, using the Mathworks MATLAB toolbox *Multibeam Radar for Adaptive Search and Track* [31]. Similar to the targets, they are simulated as nonfluctuating Swerling 0 (SW0) targets with RCS $\sigma^2 = 1$ m^2. The other parameters of the MPAR are a peak transmit power of 100 kW, an overall available bandwidth of 10 MHz, and a beamwidth of the entire phased array, when the beam is pointed at boresight, of 2° and 3° in azimuth and elevation, respectively. In the following, for all the considered radar tasks, due to the aforementioned assumptions and supposing $P_d = 0.9$ and $P_{\text{fa}} = 10^{-6}$, (2) leads to a detectability factor equal to 13.12 dB. Moreover, the noise figure is set to 5 dB.

For the tasks considered in this work, the MPAR resources are shared in order to ensure the required degree of satisfaction in performing the activities. In particular, the tracking requires to use the overall available bandwidth and PAP of the MPAR, as already mentioned, because it needs to perform object detection and tracking most accurately. Differently, for the volume search only a small portion of both the bandwidth and PAP are necessary, since it should roughly, but quickly, perform a first detection stage. Moreover, the cued search requires a higher bandwidth and PAP than the volume to refine the parameters estimate of the detected targets. As to COM, instead, its bandwidth is chosen equal to all the available bandwidth reduced by the amount employed for volume search (in fact, it is assumed that one volume look at time is performed), whereas for the PAP assignment two different

TABLE I
TASKS SIMULATION PARAMETERS

parameter	value			
	Tracking	Volume	Cued	COM
Az. beamwidth (°)	2	8	4	4
El. beamwidth (°)	3	10	5	5
bandwidth (MHz)	10	0.5	3	9.5
PAP (Wm^2)	1661.9	498.58	997.15	997.15
τ (μs)	2.5	10	5	N/A
PRF (Hz)	1500	1500	1500	N/A

strategies are performed. In the first case, it is a priori set equal to those of the cued for being easily allocated in parallel to the volume search tasks. Differently, in the second case, it is dynamically selected as specified in Section III-D in order to reach a desired channel capacity, once the distance from the receiving equipment is defined. This second strategy allows to save resources ensuring to just utilize the amount of PAP necessary to achieve the specific mission goal. Therefore, the bandwidths are set equal to 0.5 MHz for the volume search, 3 MHz for the cued search, and 9.5 MHz for the COM, whereas the PAP assignments are given in Table I, with reference to the static COM assignment, along with the main involved parameter values employed in the conducted experiments.

The PAP for the tracking task is computed from (1), with the pulsewidth τ set to 2.5 μs and pulse repetition frequency (PRF) equal to 1500 Hz. With these choices, the PAP results to be 1.66×10^3 W·m^2. Moreover, the time duration for each radar task is quantified by its dwell that is in turn obtained from the number of pulses evaluated n through (2). Differently, the duration of the COM signals is maintained constant and equal to 0.01 s. From the inspection of Table I, it is evident that the RRM can allocate cued and COM looks in parallel to volume, being the resources enough to be shared.

Other simulation parameters are the range and angular limits for the volume search, which are set equal to 75 km (range limit), $[-60°, 60°]$ (azimuth limit), and $[-30°, 0°]$ (elevation limit). Moreover, the space between adjacent beams in the volume search grid is set equal to 0.85 beamwidth fraction in both azimuth and elevation as depicted in Fig. 3. Similarly, for the COM tasks, the range limit is set equal to 20 km and the COM angular grid limits to $[-60°, 60°]$ in azimuth and $[0°, 30°]$ in elevation. Moreover, the tracking tasks are performed considering a confirmation rate equal to 20 Hz; whereas for the update tracking, the revisit time is adaptively chosen following the method based on the estimated maneuver state of Section III-C2, with the highest value set equal to 2 s and the lowest to 0.2 s. Furthermore, the update time (or time window) is set equal to a constant value of 0.05 s. Finally, as to the COM user equipment, the following parameters setting is selected, $L_s^{\text{COM}} = 27$ dB, $T_s^{\text{COM}} = 916$ K, and $A_e^{\text{rx}} = 0.7 \times 10^{-3}$ m^2.

The simulation is conducted for a total duration of 4 s and starts at time 0 s with a volume look. During the conducted simulations, tasks are scheduled respecting their priority order as well as trying to fill the update time using COM when no other task can be allocated. With respect to a given interval, the search grid can be shown together with the true

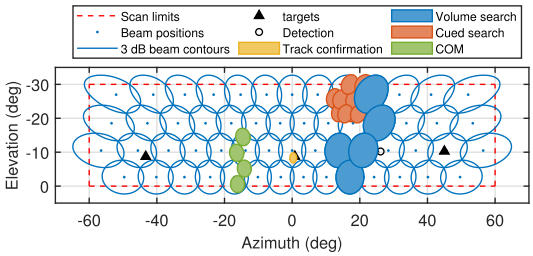

Fig. 5. Visualization of the tasks performed during the update time [0.55, 0.6] s showing the target locations and possible related detections, together with the volume search, cued search, confirmation tracking, and COM beams placed by the MPAR.

positions of the six targets, and the beams of the scheduled looks. This is shown in Fig. 5, where the visualization of the tasks performed during the update time corresponding to $[0.55, 0.6]$ s is reported showing the target locations and possible related detections, together with the volume search, cued search, confirmation tracking, and COM beams placed by the MPAR at that time window.

It is now of interest to analyze the task scheduling produced by the RRM with all the tasks executed in each update time together with their duration. To this end, Fig. 6 shows some snapshots of the timeline for the scheduled tasks along the conducted simulation. Each subplot in the figure refers to a specific update time (arranged in time-increasing order), with the specific values of the time interval on the x-axis. Interestingly, thanks to the possibility of sharing bandwidth and PAP, volume and cued search are executed in parallel as can be seen from Fig. 6(e). Similarly, COM operations are performed parallel to the volume search (in the absence of cued activities), analogously to the behavior observed in the same subplot of Fig. 6. Moreover, they also occupy in a useful way the empty time left by radar tasks, as illustrated in Fig. 6(b). As expected, the tracking tasks (both confirmation and update) are executed alone since they require all the available resources. This is evident in Fig. 6(f), (g), and (l) for the confirmation track, and in Fig. 6(h) for the track update. Finally, from the inspection of the timeline, it is also evident that the assignment is performed by the RRM adopting the priority-based scheme described in Section IV.

With reference to the above-mentioned scenario, Fig. 7 shows how tasks are executed over time and, consequently, in which way the resources are used by the MPAR. Analyzing the first subplot, it can be observed that the MPAR employs an instantaneous bandwidth that experiences some strong fluctuations. However, its average value, computed within each update interval, tends to show a more regular behavior. As expected, the occupied bandwidth is close to its maximum available value since a very high bandwidth is associated with the COM tasks (viz., 9.5 MHz) that is the task performed more frequently. The areas where the occupied bandwidth reduces correspond to the update times, where cued search areas are performed (having a bandwidth of 3 MHz). As a competitor, the algorithm of [31] is considered. It is a subcase of the proposed framework that does not perform COM operations. The results in terms of resource usage over time for the same simulation scenario are visualized in Fig. 8. With reference to

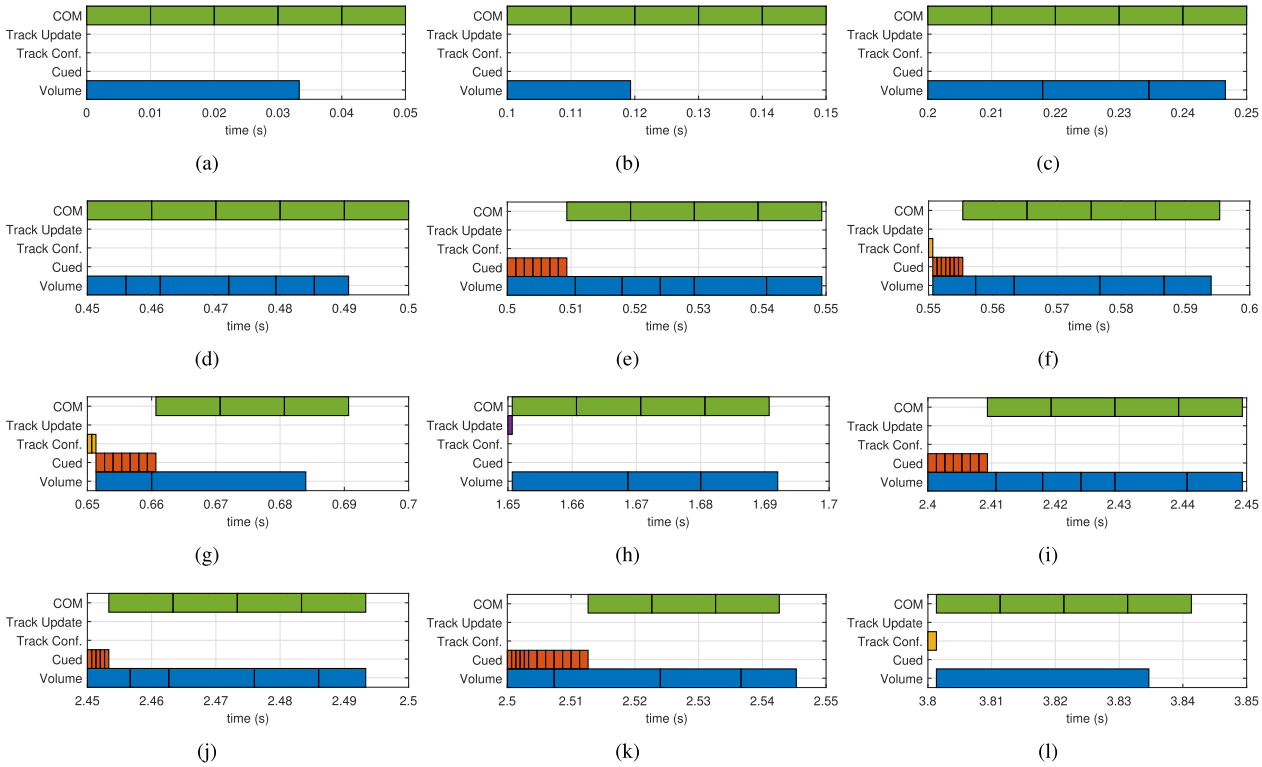

Fig. 6. Some snapshots of the timeline for the scheduled tasks along the conducted simulation from 0 to 4 s.

the bandwidth (see the first subplot of Fig. 8), it is evident that the instantaneous bandwidth continues to oscillate, whereas its average value is almost constant and close to 0.6 MHz. This result is not surprising, since it approximately corresponds to the volume search bandwidth, being it the most executed task. To have a quantitative measure of bandwidth utilization, bandwidth efficiency, defined as the average bandwidth occupancy in the overall execution time, is introduced. It is computed as the mean value of the average bandwidths over each update time. The respective values are shown in the first column of Table II (other information detailed later is also reported), where the evidence is that the proposed framework allows to increase the usage of the bandwidth resource with respect to the competitor by an amount of 89.55%–5.98% = 83.57%.

The second subplot of Figs. 7 and 8 show the utilization of the PAP in time. In both cases, the instantaneous PAPs exhibit many fluctuations over time, while their average values within each update time show more regular behaviors, with the proposed method consuming a higher PAP due to the additional COM functionalities. However, being the PAP and hence the transmitted power a precious resource, a possible variation in the assignment of the PAP-to-COM functions is also considered in this article. In particular, a dynamic allocation of the PAP is realized for the COM looks depending on the desired COM range as well as on the desired channel capacity, as described in Section III-D. Hence, Fig. 9 shows the same simulation results, but for the COM, PAP computed as in (7), setting $C_{\text{desired}} = 8$ bit/s/Hz, and randomly choosing the range at each simulating run as a realization of a uniform random variable in the interval [18, 22] km, $R_{k,\text{COM}} = \mathcal{U}[18, 22]$ km. The respective results in terms of PAP are given in the central

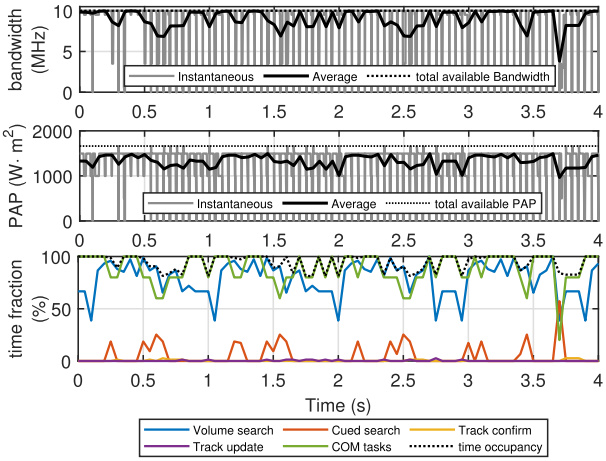

Fig. 7. Use of resources over time for the proposed scheme with a fixed PAP assignment to COM tasks. Subplots refer to bandwidth versus time (top), PAP versus time (middle), and time occupancy versus time (bottom).

subplot of Fig. 9, where the evidence is that, despite many COM looks are executed, the average PAP employed by the MPAR is almost the same as in the radar only scenario of Fig. 8.

As to the last resource, the third subplot of Figs. 7–9 emphasizes the time occupancy of the MPAR for the considered scenarios. It is computed as the ratio between the time for which at least one look is executed over the total update time and expressed as a percentage. As expected, the proposed approach (in both its versions) allows to exploit the time resource very efficiently. The time occupancy is often close to 100%, with a limited reduction in the update intervals,

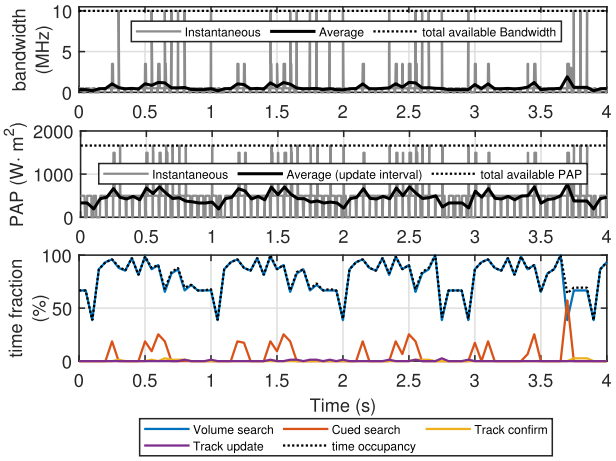

Fig. 8. Use of resources over time for the competitor not performing COM operations. Subplots refer to bandwidth versus time (top), PAP versus time (middle), and time occupancy versus time (bottom).

TABLE II
BANDWIDTH AND TIME EFFICIENCY (EXPRESSED AS A PERCENTAGE)

algorithm	value	
	bandwidth utilization (%)	time occupancy (%)
proposed strategy	89.55	94.45
method of [31]	5.98	80.02

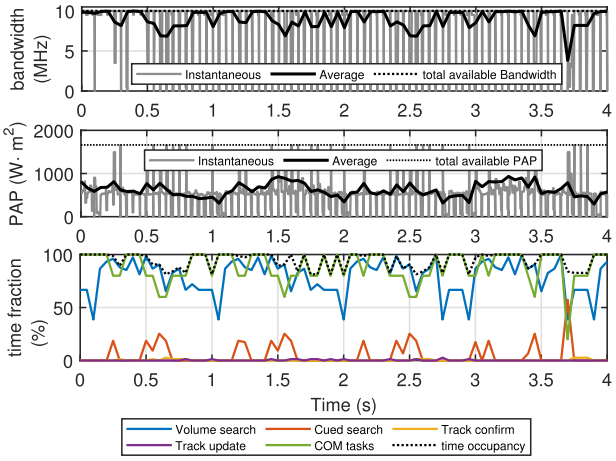

Fig. 9. Use of resources over time for the proposed scheme with a dynamic PAP allocation to COM tasks. Subplots refer to bandwidth versus time (top), PAP versus time (middle), and time occupancy versus time (bottom).

where it is not possible to allocate COM tasks to fill all the possible time gaps. Differently, from the inspection of Fig. 8, it is evident that the tasks are not optimized in the best way via the plain strategy in [31] in each update interval, with the time resource appearing to be strongly underutilized with a substantial waste of the temporal resource. Like for the bandwidth, also the time efficiency is used to glean a synthetic quantitative measure of the effectiveness of the proposed method. Specifically, it is defined as the average occupancy of time with respect to the entire observation time (expressed in percentage). The time efficiency values are also reported in Table II, with the proposed strategy showing an increment of efficiency with respect to its counterpart which passes from 80.02% to 94.45%.

VI. CONCLUDING REMARKS

In this article, the problem of task scheduling in MPAR systems performing multiple sensing and COM activities is considered. To this aim, a rule-based approach has been developed after assigning different priorities to the involved tasks and looks. Hence, the rules describing how to schedule the task looks into the timeline have been established in order to increase the bandwidth and time usage efficiency of the entire architecture. In particular, the COM operations are used along the scheduling process as gap fillers in the timeline so as to minimize the amount of time remained unused. Moreover, these looks are also organized to be executed in parallel to volume search looks in such a way that the available bandwidth at the MPAR results are almost filled. Simulation results conducted on some interesting scenarios also comprising multiple maneuvering targets have shown the benefits achievable with the proposed solution with respect to the considered competitor. In fact, both the bandwidth and time occupancy have experienced a substantial increment.

As a possible future research avenue, it would be interesting to extend the framework to dynamically distribute also the PAP between the sensing tasks.

REFERENCES

[1] P. Moo and Z. Ding, *Adaptive Radar Resource Management*. New York, NY, USA: Academic, 2015.
[2] A. Farina, A. De Maio, and S. Haykin, *The Impact of Cognition on Radar Technology*. Rijeka, Croatia: SciTech, 2017.
[3] A. Charlish and F. Katsilieris, "Array radar resource management," in *Novel Radar Techniques and Applications: Real Aperture Array Radar, Imaging Radar, and Passive and Multistatic Radar*, vol. 1. London, U.K.: SciTech, 2017, pp. 135–171.
[4] A. Charlish and F. Hoffmann, "Cognitive radar management," in *Novel Radar Techniques and Applications: Waveform Diversity and Cognitive Radar, and Target Tracking and Data Fusion*, vol. 2. London, U.K.: SciTech, 2017, pp. 157–193.
[5] A. Farina, S. Pardini, and G. Roselli, "General purpose control of a multifunctional phased-array radar," *Rivista Tecnica Selenia*, vol. 6, no. 2, pp. 12–20, 1979.
[6] D. Xu, X. Yu, D. W. K. Ng, A. Schmeink, and R. Schober, "Robust and secure resource allocation for ISAC systems: A novel optimization framework for variable-length snapshots," *IEEE Trans. Commun.*, vol. 70, no. 12, pp. 8196–8214, Dec. 2022.
[7] R. Rajkumar, C. Lee, J. Lehoczky, and D. Siewiorek, "A resource allocation model for QoS management," in *Proc. 18th Real-Time Syst. Symp.*, Dec. 1997, pp. 298–307.
[8] C.-F. Kuo, T.-W. Kuo, and C. Chang, "Real-time digital signal processing of phased array radars," *IEEE Trans. Parallel Distrib. Syst.*, vol. 14, no. 5, pp. 433–446, May 2003.
[9] C.-S. Shih, S. Gopalakrishnan, P. Ganti, M. Caccamo, and L. Sha, "Scheduling real-time dwells using tasks with synthetic periods," in *Proc. Int. Symp. System-on-Chip*, Dec. 2003, pp. 210–219.
[10] C.-S. Shih, S. Gopalakrishnan, P. Ganti, M. Caccamo, and L. Sha, "Template-based real-time dwell scheduling with energy constraint," in *Proc. 9th IEEE Real-Time Embedded Technol. Appl. Symp.*, May 2003, pp. 19–27.
[11] J. P. Hansen, S. Ghosh, R. Rajkumar, and J. Lehoczky, "Resource management of highly configurable tasks," in *Proc. 18th Int. Parallel Distrib. Process. Symp.*, Apr. 2004, p. 116.
[12] J. Hansen, R. Rajkumar, J. Lehoczky, and S. Ghosh, "Resource management for radar tracking," in *Proc. IEEE Conf. Radar*, Apr. 2006, p. 8.
[13] S. Ghosh, R. Raj Rajkumar, J. Hansen, and J. Lehoczky, "Integrated QoS-aware resource management and scheduling with multi-resource constraints," *Real-Time Syst.*, vol. 33, nos. 1–3, pp. 7–46, Jul. 2006.
[14] F. Hoffmann and A. Charlish, "A resource allocation model for the radar search function," in *Proc. Int. Radar Conf.*, Oct. 2014, pp. 1–6.
[15] A. Charlish, K. Woodbridge, and H. Griffiths, "Agent based multifunction radar surveillance control," in *Proc. IEEE RadarCon (RADAR)*, May 2011, pp. 824–829.

[16] A. B. Charlish, "Autonomous agents for multi-function radar resource management," Ph.D. thesis, Univ. College London, London, U.K., 2011.
[17] A. Charlish, K. Woodbridge, and H. Griffiths, "Multi-target tracking control using continuous double auction parameter selection," in *Proc. 15th Int. Conf. Inf. Fusion*, Jul. 2012, pp. 1269–1276.
[18] A. Charlish, F. Hoffmann, C. Degen, and I. Schlangen, "The development from adaptive to cognitive radar resource management," *IEEE Aerosp. Electron. Syst. Mag.*, vol. 35, no. 6, pp. 8–19, Jun. 2020.
[19] A. Aubry, A. De Maio, and L. Pallotta, "Power-aperture resource allocation for a MPAR with communications capabilities," 2023, *arXiv:2307.03081*.
[20] A. Aubry, A. D. Maio, and L. Pallotta, "Power-aperture product resource allocation for radar ISAC," in *Proc. IEEE Int. Workshop Technol. Defense Secur. (TechDefense)*. Rome, Italy: IEEE, Nov. 2023, pp. 1–6.
[21] D. Friedman, *The Double Auction Market: Institutions, Theories, and Evidence*. Evanston, IL, USA: Routledge, 2018.
[22] F. Katsilieris, H. Driessen, and A. Yarovoy, "Radar resource management for improved situational awareness," in *Proc. Int. Radar Conf.*, Oct. 2014, pp. 1–6.
[23] F. Katsilieris, H. Driessen, and A. Yarovoy, "Threat-based sensor management for target tracking," *IEEE Trans. Aerosp. Electron. Syst.*, vol. 51, no. 4, pp. 2772–2785, Oct. 2015.
[24] F. Katsilieris, H. Driessen, and A. Yarovoy, "Threat-based sensor management for joint target tracking and classification," in *Proc. 18th Int. Conf. Inf. Fusion (Fusion)*, Jul. 2015, pp. 435–442.
[25] W. K. Stafford, "Real time control of a multifunction electronically scanned adaptive radar (MESAR)," in *Proc. IEE Colloq. Real-Time Manag. Adaptive Radar Syst.*, 1990, pp. 1–7.
[26] J. M. Butler, "Tracking and control in multi-function radar," Ph.D. dissertation, Univ. College London, London, U.K., 1998.
[27] A. J. Orman, C. N. Potts, A. K. Shahani, and A. R. Moore, "Scheduling for a multifunction phased array radar system," *Eur. J. Oper. Res.*, vol. 90, no. 1, pp. 13–25, Apr. 1996.
[28] S. L. C. Miranda, C. J. Baker, K. Woodbridge, and H. D. Griffiths, "Phased array radar resource management: A comparison of scheduling algorithms," in *Proc. IEEE Radar Conf.*, Apr. 2004, pp. 79–84.
[29] S. Miranda, C. Baker, K. Woodbridge, and H. Griffiths, "Knowledge-based resource management for multifunction radar: A look at scheduling and task prioritization," *IEEE Signal Process. Mag.*, vol. 23, no. 1, pp. 66–76, Jan. 2006.
[30] K. Woodbridge and H. Griffiths, "Simulation methods for prioritizing tasks and sectors of surveillance in phased array radars," *Int. J. Simul., Syst., Sci. Technol.*, vol. 5, nos. 1–2, pp. 18–25, Jun. 2022.
[31] Mathworks MATLAB. *Multibeam Radar for Adaptive Search and Track*. [Online]. Available: https://it.mathworks.com/help/radar/ug/multibeam-radar-for-adaptive-search-and-track.html
[32] S. S. Blackman and R. Popoli, *Design and Analysis of Modern Tracking Systems*. Dedham, MA, USA: Artech House, 1999.
[33] S. L. C. Miranda, C. J. Baker, K. Woodbridge, and H. D. Griffiths, "Fuzzy logic approach for prioritisation of radar tasks and sectors of surveillance in multifunction radar," *IET Radar, Sonar Navigat.*, vol. 1, no. 2, pp. 131–141, 2007.
[34] S. D. Blunt and E. S. Perrins, *Radar and Communication Spectrum Sharing*. Rijeka, Croatia: SciTech, 2018.
[35] G. C. Tavik et al., "The advanced multifunction RF concept," *IEEE Trans. Microw. Theory Techn.*, vol. 53, no. 3, pp. 1009–1020, Mar. 2005.
[36] M. A. Richards, J. Scheer, W. A. Holm, and W. L. Melvin, *Principles of Modern Radar*, vol. 1. Edison, NJ, USA: SciTech, 2010.
[37] H. A. P. Blom and Y. Bar-Shalom, "The interacting multiple model algorithm for systems with Markovian switching coefficients," *IEEE Trans. Autom. Control*, vol. AC-33, no. 8, pp. 780–783, Aug. 1988.
[38] Y. Bar-Shalom, X. R. Li, and T. Kirubarajan, *Estimation With Applications to Tracking and Navigation: Theory, Algorithms and Software*. New York, NY, USA: Wiley, 2001.
[39] Y. Bar-Shalom, P. K. Willett, and X. Tian, *Tracking and Data Fusion*, vol. 11. Storrs, CT, USA: YBS, 2011.
[40] G. van Keuk and S. S. Blackman, "On phased-array radar tracking and parameter control," *IEEE Trans. Aerosp. Electron. Syst.*, vol. 29, no. 1, pp. 186–194, Jan. 1993.
[41] P. Viswanath, D. N. C. Tse, and R. Laroia, "Opportunistic beamforming using dumb antennas," *IEEE Trans. Inf. Theory*, vol. 48, no. 6, pp. 1277–1294, Jun. 2002.
[42] D. Tse and P. Viswanath, *Fundamentals of Wireless Communication*. Cambridge, U.K.: Cambridge Univ. Press, 2005.
[43] M. Kountouris, "Multiuser multi-antenna systems with limited feedback," Ph.D. dissertation, Télécom ParisTech, Paris, France, 2008.

Augusto Aubry (Senior Member, IEEE) received the Dr.-Eng. degree (Hons.) in telecommunication engineering and the Ph.D. degree in electronic and telecommunication engineering from the University of Naples Federico II, Naples, Italy, in 2007 and 2011, respectively.

From February to April 2012, he was a Visiting Researcher with Hong Kong Baptist University, Hong Kong. He is currently an Associate Professor with the University of Naples Federico II. His research interests include statistical signal processing and optimization theory, with emphasis on multi-in multi-out (MIMO) communications and radar signal processing.

Dr. Aubry was a co-recipient of the 2013 Best Paper Award (titled to B. Carlton) of IEEE TRANSACTIONS ON AEROSPACE AND ELECTRONIC SYSTEMS with the contribution "Knowledge-Aided (Potentially Cognitive) Transmit Signal and Receive Filter Design in Signal-Dependent Clutter." He was a recipient of the 2022 IEEE Fred Nathanson Memorial Award as the Young (less than 40 years of age) Aerospace and Electronic Systems Society (AESS) Radar Engineer 2022, with the following citation "For Outstanding Contributions to the Application of Modern Optimization Theory to Radar Waveform Design and Adaptive Signal Processing."

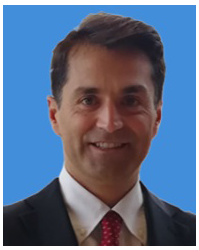

Antonio De Maio (Fellow, IEEE) received the Dr.-Eng. (Hons.) and Ph.D. degrees in information engineering from the University of Naples Federico II, Naples, Italy, in 1998 and 2002, respectively.

From October to December 2004, he was a Visiting Researcher with the U.S. Air Force Research Laboratory, Rome, NY, USA. From November to December 2007, he was a Visiting Researcher with the Chinese University of Hong Kong, Hong Kong. He is currently a Professor with the University of Naples Federico II. His research interest lies in the field of statistical signal processing, with emphasis on radar detection, optimization theory applied to radar signal processing, and multiple-access communications.

Dr. De Maio was a recipient of the 2010 IEEE Fred Nathanson Memorial Award as the Young (less than 40 years of age) Aerospace and Electronic Systems Society (AESS) Radar Engineer 2010, whose performance is particularly noteworthy as evidenced by contributions to the radar art for several years, with the following citation for "Robust CFAR Detection, Knowledge-Based Radar Signal Processing, and Waveform Design and Diversity." He was also a recipient of the 2024 IEEE Warren White Award for outstanding achievements due to a major technical advance (or series of advances) in the art of radar engineering, with the citation "For Contributions to Radar Signal Processing Techniques for Target Detection, Waveform Design, and Electronic Protection." He was a co-recipient of the 2013 Best Paper Award (titled to B. Carlton) of IEEE TRANSACTIONS ON AEROSPACE AND ELECTRONIC SYSTEMS with the contribution "Knowledge-Aided (Potentially Cognitive) Transmit Signal and Receive Filter Design in Signal-Dependent Clutter."

Luca Pallotta (Senior Member, IEEE) received the Laurea Specialistica degree (cum laude) in telecommunication engineering from the University of Sannio, Benevento, Italy, in 2009, and the Ph.D. degree in electronic and telecommunication engineering from the University of Naples Federico II, Naples, Italy, in 2014.

He was an Assistant Professor at the University of Roma Tre, Rome, Italy, from 2019 to 2022. He is currently an Assistant Professor with the University of Basilicata, Potenza, Italy. His research interests include the field of statistical signal processing, with emphasis on radar/synthetic aperture radar (SAR) signal processing, radar target detection and classification, and polarimetric radar/SAR.

Dr. Pallotta won the Student Paper Competition at the IEEE Radar Conference 2013. Since November 2020, he has been an Associate Editor of the IEEE JOURNAL OF SELECTED TOPICS IN APPLIED EARTH OBSERVATIONS AND REMOTE SENSING (JSTARS). From July 2018 to February 2021, he was an Associate Editor for the journal *Signal, Image, and Video Processing* (SIVP) (Springer).

Open Access funding provided by 'Università degli Studi di Napoli "Federico II"' within the CRUI CARE Agreement